

Manganese Complexes of 1,3,5-Triaza-7-phosphaadamantane (PTA): The First Nitrogen-Bound Transition-Metal Complex of PTA

Brian J. Frost,* Carolyn M. Bautista, Rongcai Huang, and Jason Shearer*

Department of Chemistry, MS 216, University of Nevada, Reno, Nevada 89557

Received February 24, 2006

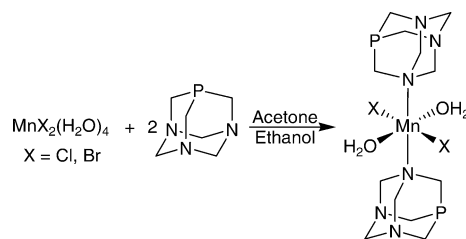
The structures of two manganese(II) complexes of 1,3,5-triaza-7-phosphaadamantane (PTA) reveal the first transition-metal complexes of PTA in which the metal preferentially coordinates to a nitrogen and not the phosphorus of PTA. The coordination environment about the manganese was probed using X-ray crystallography (solid state) and EXAFS spectroscopy (solution).

The air-stable, water-soluble, heterocyclic phosphine 1,3,5-triaza-7-phosphaadamantane (PTA)¹ has received a great deal of attention in recent years as a ligand for aqueous-phase catalysis.^{2–4} We have been interested in the coordination chemistry of PTA and, specifically, the requirements for nitrogen versus phosphorus coordination.^{5,6} PTA preferentially coordinates metals through the soft phosphorus center,

* To whom correspondence should be addressed. E-mail: Frost@chem.unr.edu (B.J.F.), shearer@chem.unr.edu (J.S.).

- (1) (a) Daigle, D. J.; Pepperman, A. B., Jr.; Vail, S. L. *J. Heterocycl. Chem.* **1974**, *11*, 407–408. (b) Daigle, D. J. *Inorg. Synth.* **1998**, *32*, 40–45.
- (2) For example, see: (a) Mebi, C. A.; Frost, B. J. *Organometallics* **2005**, *24*, 2339–2346. (b) Akbayeva, D. N.; Gonsalvi, L.; Oberhauser, W.; Peruzzini, M.; Vizza, F.; Brueggeller, P.; Romerosa, A.; Sava, G.; Bergamo, A. *Chem. Commun.* **2003**, 264–265. (c) Bolano, S.; Gonsalvi, L.; Zanobini, F.; Vizza, F.; Bertolasi, V.; Romerosa, A.; Peruzzini, M. *J. Mol. Catal. A* **2004**, *224*, 61–70. (d) Kovács, J.; Todd, T. D.; Reibenspies, J. H.; Joó, F.; Darensbourg, D. J. *Organometallics* **2000**, *19*, 3963–3969. (e) Joó, F.; Laurenczy, G.; Karady, P.; Elek, J.; Nadasdi, L.; Roulet, R. *Appl. Organomet. Chem.* **2000**, *14*, 857–859. (f) Laurenczy, G.; Joó, F.; Nadasdi, L. *Inorg. Chem.* **2000**, *39*, 5083–5088. (g) Darensbourg, D. J.; Joó, F.; Kannisto, M.; Katho, A.; Reibenspies, J. H.; Daigle, D. J. *Inorg. Chem.* **1994**, *33*, 200–208. (h) Krogstad, D. A.; Cho, J.; DeBoer, A. J.; Klitzke, J. A.; Sanow, W. R.; Williams, H. A.; Halfen, J. A. *Inorg. Chem. Acta* **2006**, *359*, 136–148. (i) Joó, F.; Nadasdi, L.; Benyei, A. C.; Darensbourg, D. J. *J. Organomet. Chem.* **1996**, *512*, 45–50. (j) Joó, F.; Laurenczy, G.; Nadasdi, L.; Elek, J. *Chem. Commun.* **1999**, 971–972. (k) Dyson, P. J.; Ellis, D. J.; Henderson, W.; Laurenczy, G. *Adv. Synth. Catal.* **2003**, *345*, 216–221.
- (3) Darensbourg, D. J.; Decuir, T. J.; Reibenspies, J. H. In *Aqueous Organometallic Chemistry and Catalysis*; Horváth, I. T., Joó, F., Eds.; High Technology; Kluwer: Dordrecht, The Netherlands, 1995; pp 61–80.
- (4) Phillips, A. D.; Gonsalvi, L.; Romerosa, A.; Vizza, F.; Peruzzini, M. *Coord. Chem. Rev.* **2004**, *248*, 955–993 and references cited therein.
- (5) Frost, B. J.; Mebi, C. A.; Gingrich, P. W. *Eur. J. Inorg. Chem.* **2006**, 1182–1189.
- (6) Frost, B. J.; Miller, S. B.; Rove, K. O.; Pearson, D. M.; Korinek, J. D.; Harkreader, J. L.; Mebi, C. A.; Shearer, J. *Inorg. Chem. Acta* **2006**, *359*, 283–288.

Scheme 1. Synthesis of Mn(OH)₂PTA₂X₂, Where X = Cl (**1**) or Br (**2**)



while the harder amine functionalities are the preferred sites of alkylation and protonation,⁴ which can be rationalized utilizing hard soft acid base (HSAB) theory. In the 3 decades since the discovery of PTA, no examples of PTA binding to a metal through nitrogen, leaving an uncoordinated phosphorus, have been observed.⁴ Darensbourg et al. described a transient intermediate tentatively identified as $[\text{Ni}(\text{PTA})_{6-n}(\text{H}_2\text{O})_n]^{2+}$ and reported as possibly containing a nitrogen-bound PTA based upon the blue color of the complex.⁷ Peruzzini et al. reported the first definitive transition-metal complex bound through a nitrogen of PTA; nitrogen coordination to silver was observed in a ruthenium-bound PTA complex (i.e., nitrogen coordination *after* metal coordination of the phosphorus).⁸ We more recently reported the first coordination complex of PTA in which only the nitrogen of PTA was bound to a hard Lewis acid (boron); the addition of BH_3 to PTA resulted in the formation of a coordination complex ($\text{PTA}-\text{BH}_3$) in which the borane was bound to nitrogen, leaving an uncoordinated phosphorus atom.⁵

Herein we present experimental data on the first nitrogen-coordinated PTA transition-metal complexes. Complexes **1** and **2** were synthesized using a procedure published for the hexamethylenetetraamine (HMT) manganese complex.⁹ The manganese salt ($\text{MnCl}_2 \cdot 4\text{H}_2\text{O}$ or $\text{MnBr}_2 \cdot 4\text{H}_2\text{O}$) was dissolved in a 1:1 acetone/ethanol (v/v) solution and added to a solution of PTA dissolved in an equal volume of ethanol and acetone (Scheme 1). Precipitation of the product with hexanes yielded

- (7) Darensbourg, D. J.; Robertson, J. B.; Larkins, D. L.; Reibenspies, J. H. *Inorg. Chem.* **1999**, *38*, 2473–2481.
- (8) Lidrissi, C.; Romerosa, A.; Saoud, M.; Serrano-Ruiz, M.; Gonsalvi, L.; Peruzzini, M. *Angew. Chem., Int. Ed.* **2005**, *44*, 2568–2572.
- (9) Tang, Y.-C.; Sturdivant, J. H. *Acta Crystallogr.* **1952**, *5*, 74–82.

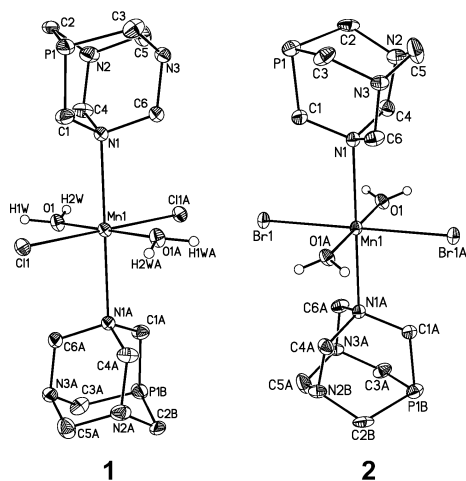


Figure 1. Thermal ellipsoid plots (50% probability) showing the molecular structures of **1** and **2**. Hydrogen atoms have been omitted from the PTA ligands for clarity.

Table 1. Selected Bond Lengths [Å] and Angles [deg] for **1–3**

	1	2	3
Mn–X	2.4974(4)	2.6603(3)	2.6398(4) ^c
Mn–O	2.1581(12)	2.1398(19)	2.167(9) ^c
Mn–N	2.4552(14)	2.4776(2)	2.458(11) ^c
P1–C _{ave}	1.825(4) ^a	1.817(5) ^a	—
N1–C _{ave}	1.484(2) ^a	1.488(4) ^a	1.490(5) ^a
N2–C _{ave}	1.474(4) ^a	1.483(8) ^a	1.476(5) ^a
N3–C _{ave}	1.470(2) ^a	1.471(4) ^a	1.466(2) ^a
N–Mn–N	180.0 ^b	180.0 ^b	179.22(5)
O–Mn–O	180.00(7)	180.0 ^b	178.66(6)
X–Mn–X	180.0 ^b	180.0 ^b	178.771(13)
O–Mn–N	92.39(5)	92.05(7)	90.38(5), 88.65(5)
N–Mn–X	91.49(3)	91.61(5)	90.17(4)
O–Mn–X	90.78(4)	90.25(6)	90.44(4)

^a Average of three values. ^b Crystallographically defined as 180°. ^c Average of two values.

clear colorless crystals in 85% yield. Also presented is the solid-state structure of the HMT analogue $\text{MnBr}_2(\text{OH}_2)_2\text{-(HMT)}_2$ (**3**).

The solid-state structures of **1** and **2** were determined by X-ray crystallography (Figure 1).¹⁰ The two complexes are isomorphous, with the manganese(II) lying on an inversion center in an octahedral environment with two water, two halide, and two nitrogen-bound PTA ligands all in a mutually trans arrangement (Table 1). In both compounds **1** and **2**, P1 and N2 exhibit occupational disorder, which has been modeled in the final refinement.¹⁰ The N1–C and P1–C distances are 1.484(2) and 1.825(4) Å, respectively, consistent with other PTA structures.⁴ In both **1** and **2**, N3 is locked into place through the formation of an intermolecular hydrogen bond to a manganese-coordinated water molecule, $\text{O1}\cdots\text{N3} = 2.7554(19)$ Å (Figure 2). A second hydrogen bond between the manganese-bound water and a halogen on an adjacent manganese center is also observed; $\text{O1}\cdots\text{Cl} = 3.1558(14)$ Å for **1**, and $\text{O1}\cdots\text{Br} = 3.302(2)$ Å for **2**. Unlike protonation or alkylation of PTA, which results in elongation of the (N)C–N bond,^{3,4} metalation of a PTA nitrogen results in little or no change in the (N)C–N distance relative to the unbound nitrogen centers. The lack of a significant C–N bond elongation is consistent with compound **3**, where the N1–C_{ave} distances are only slightly

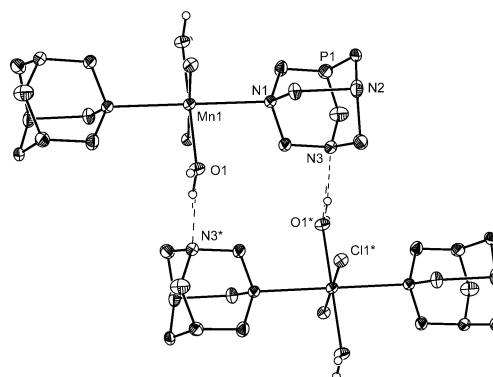


Figure 2. Thermal ellipsoid representation (50% probability) of **1** depicting the hydrogen bonding observed between the PTA ligands and the manganese-coordinated water molecules, $\text{O1}\cdots\text{N3} = 2.7554(19)$ Å (* indicates atoms at equivalent positions, $x + 1, y, z$).

longer with respect to the N–C distances of the unbound nitrogen centers (vide infra). Manganese EXAFS analyses of solid samples of both **1** and **2** are consistent with the crystallographically derived structures.¹¹

For comparison, we have determined the solid-state structure of the HMT adduct **3**.¹⁰ The chloride complex $[\text{MnCl}_2(\text{OH}_2)_2(\text{HMT})_2]$ has been previously reported.⁹ Complexes **1–3** are virtually identical in structure. The Mn–N bond lengths of the three complexes are within 0.02 Å of each other, and the Mn–O distances are within 0.03 Å. Other bond lengths and angles are also similar (see Table 1), with any differences the result of substitution of bromine for chlorine or phosphorus for nitrogen. Complex **3** is held together by a more complex set of intermolecular hydrogen bonds compared to **1** and **2**; each HMT ligand forms two hydrogen bonds [$\text{O}\cdots\text{N} = 2.798(2)\text{–}2.866(2)$ Å] to manganese-bound water molecules.¹¹

In solution, complexes **1** and **2** exist as a series of substitutional isomers. EXAFS data (vide infra) suggest that the halide ligands in **1** and **2** dissociate in water, forming a mixture of water and PTA-bound compounds, such as $[\text{Mn}(\text{OH}_2)_4\text{PTA}_2](\text{Cl})_2$. Electrospray ionization mass spectrometry of **2** reveals a variety of substituted complexes including $[\text{MnBr}(\text{OH}_2)_2\text{PTA}_2]^+$ and $[\text{MnBr}(\text{OH}_2)_2\text{PTA}_3]^+$. As a result of the paramagnetic nature of the d^5 manganese(II) center, no NMR spectra could be obtained. The addition of excess

(10) Crystallographic data were collected at $100(\pm 1)$ K on a Bruker APEX CCD diffractometer with Mo K α radiation ($\lambda = 0.7107$ Å). Crystal data for compound **1** (CCDC 293763): $\text{C}_{12}\text{H}_{28}\text{N}_6\text{O}_2\text{P}_2\text{Cl}_2\text{Mn}$, MW = 476.18, $T = 100(2)$ K, $\lambda = 0.71073$ Å, monoclinic, $P2_1/c$, $Z = 2$, $a = 7.3338(9)$ Å, $b = 6.3291(8)$ Å, $c = 20.950(3)$ Å, $\alpha = 90^\circ$, $\beta = 96.703(2)^\circ$, $\gamma = 90^\circ$, $V = 965.8(2)$ Å³, 16 271 measured reflections, 7451 independent reflections ($R_{\text{int}} = 0.0369$), $R1 = 0.0350$, and $wR2 = 0.0654$. Crystal data for compound **2** (CCDC 293764): $\text{C}_{12}\text{H}_{28}\text{N}_6\text{O}_2\text{P}_2\text{Br}_2\text{Mn}$, MW = 565.10, $T = 100(2)$ K, $\lambda = 0.71073$ Å, monoclinic, $P2_1/c$, $Z = 2$, $a = 7.3749(4)$ Å, $b = 6.5706(3)$ Å, $c = 20.7553(11)$ Å, $\alpha = 90^\circ$, $\beta = 96.817(2)^\circ$, $\gamma = 90^\circ$, $V = 998.64(9)$ Å³, 10 062 measured reflections, 3521 independent reflections ($R_{\text{int}} = 0.0510$), $R1 = 0.0392$, and $wR2 = 0.0717$. An occupational disorder between P1 and N2 exists in the structures of both compounds **1** (71/29%) and **2** (58/42%) and was modeled appropriately. Crystal data for compound **3** (CCDC 293765): $\text{C}_{12}\text{H}_{28}\text{N}_6\text{O}_2\text{Br}_2\text{Mn}$, MW = 531.18, $T = 100(2)$ K, $\lambda = 0.71073$ Å, orthorhombic, $Pna2_1$, $Z = 4$, $a = 21.9004(9)$ Å, $b = 7.2807(3)$ Å, $c = 11.8634(5)$ Å, $\alpha = \beta = \gamma = 90^\circ$, $V = 1891.62(14)$ Å³, 32 391 measured reflections, 6722 independent reflections ($R_{\text{int}} = 0.0322$), $R1 = 0.0219$, and $wR2 = 0.0491$.

(11) See the Supporting Information for details.

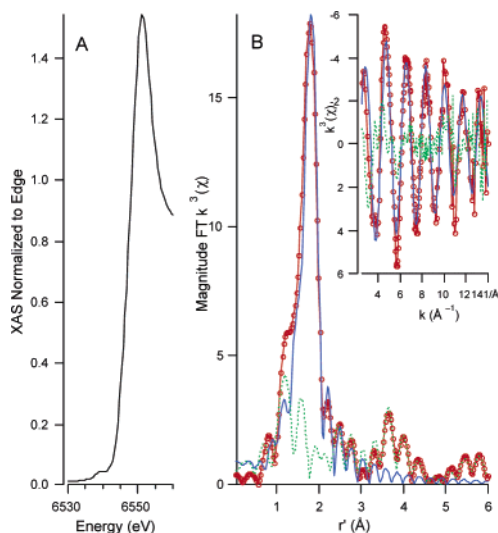


Figure 3. Manganese K-edge XAS data for the frozen solution of **1**. (A) Edge region of the manganese K-edge spectrum. (B) Magnitude FT $k^3(\chi)$ depicting the real data (connected circles), best fit to the data (solid line), and difference spectrum (dashed line). The inset shows $k^3(\chi)$ depicting the real data (connected circles), best fit to the data (solid line), and difference spectrum (dashed line).

PTA to a solution of **1** resulted in no observable ^{31}P NMR spectrum, indicating rapid exchange of the PTA ligands in water.

Manganese K-edge X-ray absorption spectroscopic (XAS) studies were performed on aqueous frozen solutions of **1** and **2** at 20 K.¹² Both solution samples yielded virtually identical spectra. The preedge regions for both spectra display peaks at ~ 6539 eV, which are assigned to $1s \rightarrow 3d$ transitions. These transitions are relatively weak [0.09(3) eV relative to the edge for **1** and 0.10(2) eV relative to the edge for **2**] and are consistent with a parity-forbidden $1s \rightarrow 3d$ transition (i.e., six-coordinate manganese in nominal O_h or D_{4h} symmetry). The positions of the edge jumps for both **1** and **2** are consistent with those of manganese(II).¹³ Refinements to the EXAFS region for both complexes are also consistent with those of six-coordinate manganese centers (Figure 3 and the Supporting Information).

In line with the X-ray crystallographic and solid-state XAS data, we find no evidence that phosphorus is contained within the primary coordination sphere of frozen solutions of either **1** or **2**. However, we also find no evidence that the halides are ligated to the manganese centers, suggesting that these ligands dissociate upon dissolution of the complexes and are most likely displaced by water. An initial refinement to the EXAFS region of **1** utilized a model containing one nitrogen

shell with two scatterers and one oxygen shell containing four scatterers. Although this model gave a reasonable GOF (1.03), the nitrogen shell was highly disordered [$\sigma^2 = 0.014$ –(8) \AA^2]. It was felt that the disorder was unreasonably large for an inner-sphere scatterer. Refinement of the EXAFS data for **1** modeled as a hexaqua species resulted in a poorer GOF value (1.45). We were able to obtain an excellent fit to the solution-state EXAFS region of **1** by modeling the data as a mixture of substitutional isomers. To model the data as a mixture of six-coordinate N/O-ligated manganese complexes, we employed a phase and amplitude functional constructed from a mixture of nitrogen and oxygen scatterers (the N/O shell). Utilization of this functional thus allows us to approximate a complex mixture of substitutional isomers present in solution as a “single” six-coordinate species. We thus refined the EXAFS data for **1** using two N/O shells; one shell containing two N/O scatterers at 2.319(9) \AA and one shell containing four N/O scatterers at 2.193(3) \AA . The best fit to the EXAFS region for **2** is virtually identical with that of **1** [four N/O scatterers at 2.194(2) \AA ; two N/O scatterers at 2.300(5) \AA]. These results support the supposition that ligand substitution for both **1** and **2** is facile in solution and a variety of substitutional isomers are produced upon dissolution.

In conclusion, we have reported here the first example of a PTA complex bound to a transition metal (manganese) through nitrogen. The complexes described have been characterized by X-ray crystallography, EXAFS, and mass spectrometry. On the basis of the data reported here and reports of others,^{5,7,8} it appears that nitrogen-bound PTA complexes might not be as unusual as previously thought. HSAB theory may be used to help predict which binding site on PTA a Lewis acid will preferentially coordinate; for example, the very hard manganese(II) center proved to be an ideal choice for the synthesis of a nitrogen-bound PTA complex. Presently, our group is exploring other metals that may exhibit a propensity to bind PTA through nitrogen.

Acknowledgment is made to the donors of the American Chemical Society Petroleum Research Fund for partial support of this project. The authors also thank V. J. Catalano for help in handling the crystallographic disorder and the Department of Chemistry at the University of Nevada for support. Financial support from the National Science Foundation is acknowledged for the X-ray diffractometer (Grant CHE-0226402). Use of the National Synchrotron Light Source, Brookhaven National Laboratory, was supported by the U.S. Department of Energy office of basic energy science under Contract DE-AC02-98CH10886.

Supporting Information Available: Detailed experimental procedures, IR spectra of **1** and **2**, crystallographic files in CIF format, thermal ellipsoid representation of **3**, packing diagrams for **1**–**3**, details of the X-ray absorption studies, refinements to solid-state and solution spectra for **1** and **2**, plots of $k^3(\chi)$ and Fourier transform (FT) $k^3(\chi)$ for the solution spectrum of **2** and solid-state spectra of **1** and **2**. This material is available free of charge via the Internet at <http://pubs.acs.org>.

(12) EXAFS spectra were recorded at the National Synchrotron Light Source (Brookhaven National Laboratories, Upton, NY) on Beamline X9b. Spectra were recorded as fluorescence data and are the averaged sum of three data sets. Data analysis was performed with the XAS refinement package EXAFS123 provided by Prof. Robert C. Scarrow (Haverford College, Haverford, PA): Egdal, R. K.; Hazell, A.; Larsen, F. B.; McKenzie, C. J.; Scarrow, R. C. *J. Am. Chem. Soc.* **2003**, *125*, 32–33 and references cited therein. We present refinements based on unfiltered k^3 data (see the Supporting Information). We note that refinements based on Fourier-filtered data (FT from 2.2 to 14.3 \AA^{-1} ; back-transformation from 1.0 to 3.0 \AA^{-1}) yielded nearly identical results.

(13) Farges, F. *Phys. Rev. B* **2005**, *71*, 155109-1–155109-14.